

How crosslink numbers shape the large-scale physics of cytoskeletal materials

Sebastian Fürthauer¹ and Michael J. Shelley^{1,2}

¹Center for Computational Biology, Flatiron Institute, New York, NY 10010, USA

²Courant Institute, New York University, New York, NY 10012, USA

Cytoskeletal networks are the main actuators of cellular mechanics, and a foundational example for active matter physics. In cytoskeletal networks, motion is generated on small scales by filaments that push and pull on each other via molecular-scale motors. These local actuations give rise to large scale stresses and motion. To understand how microscopic processes can give rise to self-organized behavior on larger scales it is important to consider what mechanisms mediate long-ranged mechanical interactions in the systems. Two scenarios have been considered in the recent literature. The first are systems which are relatively sparse, in which most of the large scale momentum transfer is mediated by the solvent in which cytoskeletal filaments are suspended. The second, are systems in which filaments are coupled via crosslink molecules throughout. Here, we review the differences and commonalities between the physics of these two regimes. We also survey the literature for the numbers that allow us to place a material within either of these two classes.

I. INTRODUCTION

Living systems move. On cellular scales this motion is actuated by networks of polymer filaments crosslinked by molecular-scale motors that exert forces between them. This system is collectively referred to as the cytoskeleton [1, 2]. Understanding how the material properties of the cytoskeleton emerge from the properties of cytoskeletal components is one of the great challenges for soft condensed matter physics and cell biology [3]. Solving it will allow biologists to predict the effects of molecular scale perturbations on cellular organelles and enable physicists and engineers to pursue strategies for developing similarly complex and robust materials in the lab. Here, we take measure of the current state of theory for understanding the emergent physics of cytoskeletal systems based on filament scale interactions.

Symmetry based theories have helped clarify the fields, such as densities, velocities and order parameters, through which the dynamics of active materials can be described on long length and time scales [4–6]. These theories have also provided means for generating a more or less complete list of material properties (or phenomenological coefficients), such as viscosities, elastic moduli, and activity coefficients which characterize a material. While this type of information can be used to relate the effects of molecular perturbations to material properties [7], they do not address the question how micro-scale processes set the large-scale physics.

To approach this challenge physicists and mathematicians have generalized the methods developed for polymeric and liquid crystalline systems [8, 9], and Boltzmann’s statistical physics for gases, to incorporate the effects of the microscopic activity of molecular-scale motors. These efforts have led to a set of theories which describe relatively sparsely connected polymeric assemblies whose large scale behavior is dominated by momentum transfer via solvent flows [10–12]. In parallel, other groups have extended the physics of elastic networks to obtain theories for the physics of crosslinked materials on time scales that are short compared to crosslinker dynamics [13].

However, recent work has increased the awareness that many cytoskeletal systems, belong to a third class of active materials. They are highly crosslinked gels, in which filaments are transiently coupled by a large number of motors and crosslinks, which bind and unbind on time scales that are fast compared to the long time, large scale dynamics of the system. This highly crosslinked regime is set apart by new physical phenomena. Most strikingly, filaments in highly crosslinked systems can slide through the gel at speeds that are independent of the structure of their local surrounding. This phenomenon has been predicted theoretically and observed *in vitro* [14], and *in vivo* [15–17]. Theories for highly crosslinked systems take inspiration from early work on actin bundles [18, 19] and describe larger networks that are crosslinked by molecular motors with different symmetries and force velocity relations [20].

The goal of this review is to give a perspective on our current understanding of the physics of cytoskeletal materials. We highlight the differences between highly and sparsely crosslinked cytoskeletal networks, and their models. Where possible from published data, we will classify known examples along these lines. Along the way we will identify and highlight some open challenges that the field needs to address in order to enable a quantitative and predictive physics of these living materials.

In this review, we focus on continuum models and the microscopic models underlying their derivations. We do however emphasize that symmetry based theories [21], continuum models obtained by coarse graining microscopic models [22, 23], and agent based models for the same systems [24–27] have been extensively studied in numerical simulations as well.

In section II we review the key constituents of cytoskeletal. Then, in section III we propose a classification of cytoskeletal structures as either highly or sparsely crosslinked. To guide us in this, we review the conditions under which

a materials long-range momentum transport is dominated by crosslink interactions or by solvent flow, respectively. We then classify studied cytoskeletal materials given published data. After that, in Section IV, we review the theoretical descriptions of both highly and sparsely crosslinked materials, highlighting and contrasting their different physics. We point out how these differences can be used both as a predictive and diagnostic tools.

II. KEY CONSTITUENTS OF THE CYTOSKELETAL NETWORKS

The cytoskeleton is the cellular machinery which enables cells to do mechanical work on their organelles and on their surroundings. The cytoskeleton consists of polymer filaments, proteins that crosslink and actuate these filaments,

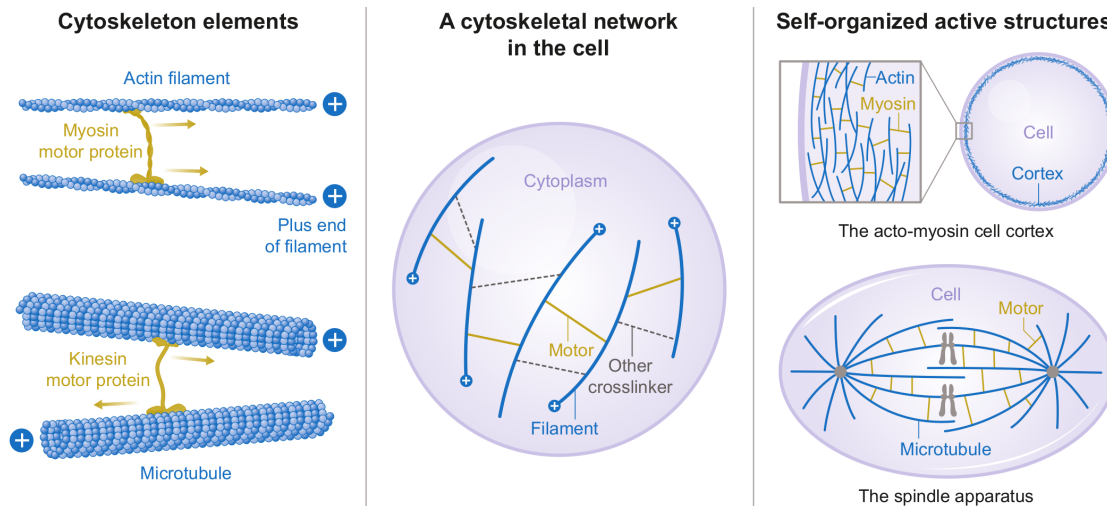


FIG. 1: Polar cytoskeletal filaments are coupled and actuated by molecular scale motors (left). Collectively they form the cytoskeletal networks (middle) which are the materials that make up many important biological structures (right).

and regulators which help organize and coordinate their functions in time and space. All of these constituents are suspended in cytoplasm, which is the aqueous slurry that makes up a cell's interior.

A. Cytoskeletal Filaments

Several types of cytoskeletal filaments exist. The two most studied and most abundant ones are filamentous actin and microtubules [2]; see Fig. (1). Both are structurally polar, meaning that their molecular structure differentiates one direction from the other. They are both transient since they are constantly assembling and disassembling. They are active since filament assembly and disassembly are driven by energy derived from GTP. While for our purposes here, it is sufficient to think of cytoskeletal filaments as polar rods, we want to emphasize that in typical *in vivo* systems the lifetime of actin filaments and microtubule is often much shorter than the time scale of large scale rearrangements of the system. One typical example is gastrulation in fruitfly. This process, that is driven by actomyosin contractions, takes about 2 hours and is driven by actomyosin, which turns over within minutes [28]. Another such process is the separation of chromosomes during cell division in the nematode worm *C. elegans*, which takes tens of minutes and is achieved by microtubules that have lifetimes of tens of seconds [29]. There are additional cytoskeletal filaments beyond actin and microtubules, largely called intermediate filaments. Examples include keratins, which are a large family of proteins that encompass vimentins, which play a role in cell motility, and lamins, which act as a mechanical scaffolding for the cell nucleus. These intermediate filaments - so-called since their thickness in the electron tomographs where they were first characterized was between that of thin actin filaments and that of thick Myosin mini-filaments - are typically longer-lived, apolar, and are hypothesized to provide cells with long time elasticity. Kinesins, myosins and dyneins that link intermediate filaments to the microtubule and actin cytoskeleton have been identified, but so far their role remains under-explored.

B. Active and passive crosslinkers

The second class of molecules that are important for the cytoskeleton are crosslinking proteins which connect cytoskeletal filaments to each other and to other structures such as chromosomes and membranes. Too many types exist to do them justice in a review focussed on the physics of the cytoskeleton, so we refer the reader to [30] and [31] for recent perspectives on actin and microtubule associated crosslinkers. Many of these crosslinkers are molecular scale motors. This means they have access to a chemical fuel reservoir - in general Adenosine-Tri-Phosphate (ATP) - from which they can draw power to do mechanical work upon the structures they crosslink. Motors can walk along cytoskeletal filaments, acting as moving crosslinks, which slides filaments past each other. Or, they can carry a cargo, like a vesicle or a mitochondrion, along filaments. The most abundant actin-associated molecular motors are myosins. The most abundant microtubule-associated ones are dyneins and kinesins. Typically motors can exert forces of up to several pico-Newtons, and their unloaded walking speeds on filaments can vary from nanometers to microns per second. Finally, motors can be more or less processive. A motor's processivity measures the expected number of steps a motor typically takes, before it unbinds from the filament to which it is attached [1, 2].

C. Cytoplasm

The last important actor in understanding the physics of the cytoskeleton is the aqueous slurry in which it is immersed. While the rheology of the cytoplasm is most certainly complex [32], most current physical theories for the cytoskeleton ignore this fact - mainly because the detailed characteristics of cytoplasmic rheology are poorly understood and difficult to model. The theories that we review, thus approximate it as a very viscous Newtonian fluid with a viscosity between 100 and 1000 times that of water; see for example [33].

D. Forces and torques in cytoskeletal networks

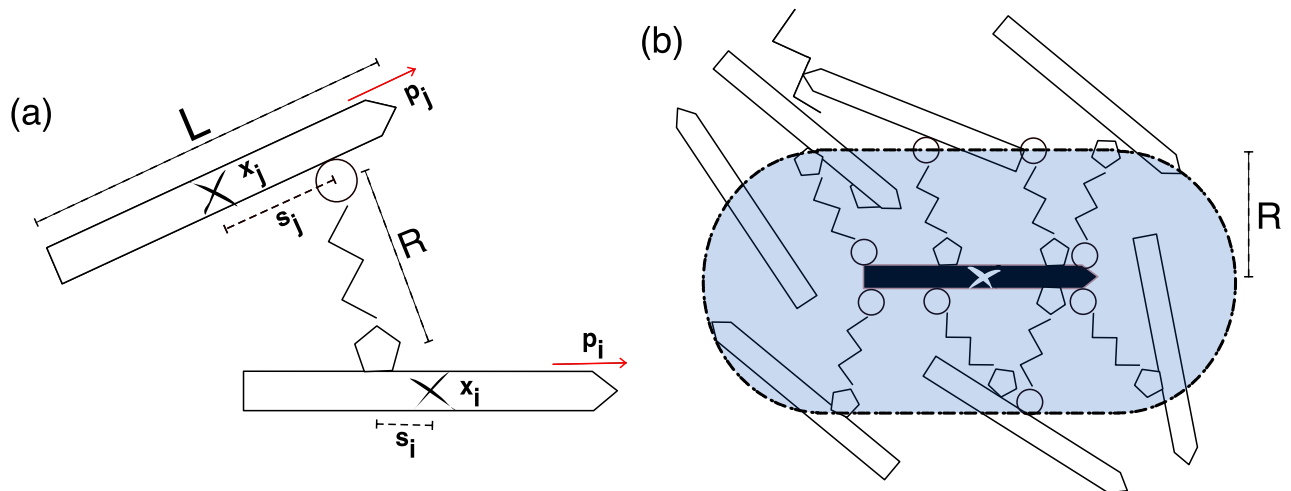


FIG. 2: (a) Interaction between two cytoskeletal filament i and j via a molecular motor. Filaments are characterized by their positions $\mathbf{x}_i, \mathbf{x}_j$, their orientations $\mathbf{p}_i, \mathbf{p}_j$, and connect by a motor between arc-length position s_i, s_j . A motor consist of two heads that can be different (circle, pentagon) and are connected by a linker (black zig-zag) of length R (b) The total force on filament i is given by the sum of the forces exerted by all a (circle) and b (pentagon) heads, which connect the filament into the network. The shaded area shows all geometrically accessible positions that can be crosslinked to the central (black) filament.

The goal of a physical theory for the cytoskeleton is to predict how filaments in a cytoskeletal network rearrange in response to the forces that they experience and produce. The larger goal is a quantitative understanding of the mechanical processes that allow cytoskeletal structures to self-organize and perform their complex tasks within cells.

The elementary starting point is characterizing the total force \mathbf{F}_i that acts on the i -th filament in the network. We

assume that it has the form

$$\mathbf{F}_i = \sum_j \mathbf{F}_{ij}^\times + \mathbf{F}_i^s = 0, \quad (1)$$

which vanishes since cytoskeletal systems are overdamped; see Fig. 1 (middle). The total force on each filament consists of crosslink mediated forces $\sum_j \mathbf{F}_{ij}^\times$ and a contribution \mathbf{F}_i^s , which comes from the drag between filaments and a moving solvent. The crosslink mediated force between filaments i and j is given by

$$\mathbf{F}_{ij}^\times = \int_{-L/2}^{L/2} ds_i \int_{-L/2}^{L/2} ds_j \int_{\Omega(\mathbf{x}_i + s_i \mathbf{p}_i)} d^3x \delta(\mathbf{x} - \mathbf{x}_j - s_j \mathbf{p}_j) \mathbf{f}_{ij}, \quad (2)$$

where \mathbf{f}_{ij} is the force density exerted by crosslinkers between the arclength positions s_i and s_j on the two filaments i, j , respectively; see Fig. 2. Here, $\Omega(\mathbf{x})$ is a sphere centered around the point \mathbf{x} and whose radius R is the size (maximal extension) of the cross-linker. Here all filaments are taken to have the same length L . Analogous expressions for the torques and total torque on filament i hold.

In the following we will argue that modeling of cytoskeletal networks has focussed on two different regimes: (i) a highly crosslinked regime in which the long range momentum transport through the gel is dominated by crosslinking forces and (ii) a regime in which momentum transport through the solvent dominates. Theories for the two limits make very different predictions for the scaling of important material properties and dynamics.

III. WHICH CYTOSKELETAL MATERIALS ARE HIGHLY CROSSLINKED?

We now discuss the crossover between the highly and sparsely crosslinked regimes and try to classify a few well studied cytoskeletal systems along these lines. For this we define the density of cytoskeletal filaments $\rho = \sum_i \delta(\mathbf{x}_i - \mathbf{x})$ and the force density $\mathbf{f} = \sum_i \delta(\mathbf{x}_i - \mathbf{x}) \mathbf{F}_i$. Since crosslink mediated interaction are short ranged we can write

$$\mathbf{f} = \nabla \cdot \boldsymbol{\Sigma} - \Gamma \rho (\mathbf{v} - \mathbf{v}^s) + \mathcal{O}(L^4) = 0, \quad (3)$$

where L is assumed small compared to the system scale [20]. In the following we use the word gel to signify the filaments and crosslinks and solvent for the cytoplasm in which they are immersed. The gel stress $\boldsymbol{\Sigma}$ encodes the momentum flux through the crosslinks which connect filaments, and $\Gamma \rho$ is the friction coefficient between the gel and the solvent. Finally, \mathbf{v} and \mathbf{v}^s are the gel and solvent center of mass velocities, respectively. If we take the solvent to be a Newtonian fluid with viscosity μ it obeys the Stokes equation

$$\mu \Delta \mathbf{v}^s - \nabla \Pi^s + \Gamma \rho (\mathbf{v} - \mathbf{v}^s) = 0, \quad (4)$$

where Π^s is the hydrostatic pressure. The characteristic length scale over which momentum is transported through the solvent, the permeation length, is thus given by

$$\ell^s = \sqrt{\frac{\mu}{\rho \Gamma}}, \quad (5)$$

which decreases as the density ρ of filaments in the gel increases. Conversely, crosslinks generate friction between the filaments they connect, which leads to a viscous contribution $\mu^g \rho^2 \nabla \mathbf{v}$ to $\boldsymbol{\Sigma}$, i.e. proportional the strain rate of the gel and to the number of filament-filament interactions mediated by crosslinks [14, 20]. Here $\mu^g \rho^2$ is the gel viscosity. Thus we expect the typical length scale over which momentum is transported through the gel to be

$$\ell^g = \sqrt{\frac{\mu^g \rho^2}{\Gamma \rho}}, \quad (6)$$

which increases with filament density. The implied assumption of this calculation is that the number of realized crosslink connections is limited by the number of geometrically possible filament-filament interactions and not the number of crosslinking molecules available. It can however easily be generalized.

In the following we consider a system highly crosslinked if $\ell^g \gg \ell^s$ and sparsely crosslinked if $\ell^s \gg \ell^g$. We next review the literature and overview which cytoskeletal systems are highly or sparsely crosslinked, respectively; see Fig. 3.

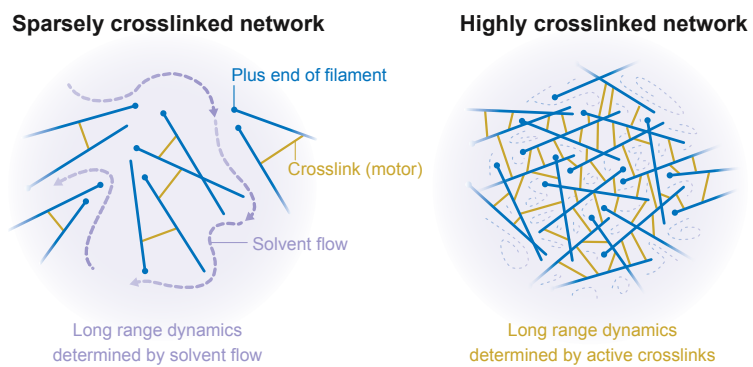


FIG. 3: Illustration of the key differences between highly and sparsely crosslinked networks, emphasizing the dominant mechanisms of large scale momentum transport.

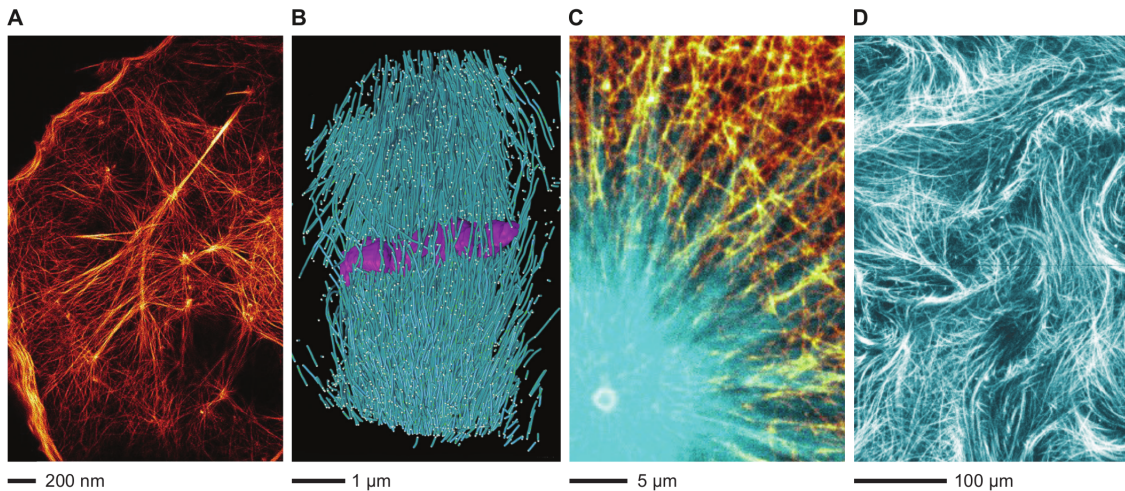


FIG. 4: Biological and artificial cytoskeletal networks: (A) SIM-TIRF super-resolution microscopy image of the actin cortex from a kidney culture cell. With permission from [34]. (B) Electron tomography reconstruction of the inner spindle microtubules of an embryonic *C. elegans* mitotic spindle. Taken from [29]; (C): spinning disk fluorescence microscopy image of microtubules and actin in a *Xenopus laevis* interphase aster in egg extract. Courtesy of James Pelletier; (D) snapshot from an experiment of an active microtubule nematic synthesized from engineered multimeric kinesin-1 motors and stabilized microtubules. Adapted with permission from [35]. Throughout the figure actin filaments are represented in orange and microtubules in blue.

A. The cell cortex

The cell cortex is a thin layer of actin filaments that localize at the cell membrane; see Fig. 4 (A). It is actuated by non-muscle myosin 2 and held together by a variety of crosslinkers and proteins which regulate assembly and disassembly of both thick (myosin) filaments and thin (actin) filaments [30]. Typically the thickness of the cortical layer is 300-1000nm [36]. Flow of actomyosin is vital for cell polarity establishment (the process by which cells break the symmetry between two daughter cells) [37, 38], cell migration and shape changes [39], cell division [40], as well as regulating cellular surface tension [41]. On time-scales longer than filament lifetimes, the cell cortex is well described as an active fluidic material [7, 37, 42].

Comprehensive estimates of the numbers of crosslinks in the actin cell cortex are hard to come by. That said, many actin filaments are nucleated by the nucleator Arp2/3 which is a crosslinker itself. In [43] the authors estimate that roughly nine out of ten actin filaments are nucleated by Arp2/3, while about one out of ten is nucleated by formins. This finding suggests that the actin cortex is highly crosslinked starting from its nucleation. Moreover, actin filaments are actively crosslinked by myosin motors and other crosslinkers. In [44] the authors count the numbers of the most important actin binding partners in fission yeast cells. They find that the number of crosslinkers and motors acting on actin filaments is comparable (or larger) than the number of nucleators (Arp2/3 and formins) in the system. Thus, if one estimates that the number of filaments is roughly proportional to the number of available nucleators, one concludes that there are several crosslinking interactions per filament exist at any give time. That is, the actin cortex is highly crosslinked.

B. The spindle

The spindle is the cellular apparatus which segregates chromosomes during cell division. Its main constituents are microtubules which are crosslinked and actuated by dynein and kinesin molecular motors; see Fig. 4 (B). Despite having common constituents and function, spindle structure can vary widely, even in a single organism.

One spindle whose physics has been studied extensively is the meiotic spindle of *Xenopus laevis*. This spindle can be reconstituted in frog egg extract, which makes it particularly attractive to study *ex vivo*. These spindles are large - about 50 microns long - and consist of microtubules whose lengths and lifetimes are exponentially distributed around an average length and lifetime of about 6 microns and 20 seconds, respectively [45]. They have been shown to obey the fluctuation spectra expected for active nematic gels [46]. In these spindles, microtubules nucleate by an auto-catalytic mechanism in which pre-existing microtubules recruit growth factors that initiate the formation of new microtubules [47–51]. This mechanism implies that filaments are created crosslinked to the spindle gel. The details

of the pathway controlling nucleation have been investigated [52, 53]. The motor proteins dynein and Eg-5 kinesin crosslink the spindle network further. While direct measurements of the number of Eg-5 kinesin crosslinks are not available, observations of microtubule motion in spindles allow an estimate. In [17] the authors quantify the motion and polarity of microtubules in *Xenopus* spindles. They estimate that two or more motors per filament are required to explain experimental observation that velocity fluctuation are highly correlated throughout the whole spindle. In our language this means that ℓ^g is comparable to system size and thus that the *Xenopus* spindle is highly crosslinked.

Another well studied spindle is the embryonic mitotic spindle of the nematode worm *C. elegans*. These spindles are much smaller - $10\mu\text{m}$ pole to pole - and have been fully reconstructed using electron tomography [29]; see Fig. 4 (C). Using this structural information, together with light microscopy and mathematical modelling, the authors in [54] argue that the connection between spindle poles and chromosomes is indirectly maintained by microtubules crosslinking to other microtubules. While the evidence is indirect it is suggestive of a highly crosslinked network.

The third example that we want to highlight here is the female meiotic spindle, also in *C. elegans*. This spindle is about half the size of the mitotic one and has also been reconstructed in tomography. The findings from tomography studies [55, 56] suggest that it consists of short and short-lived microtubules and is structurally quite similar to the *Xenopus laevis* meiotic spindle. It is thus tempting to speculate that this spindle too is a highly crosslinked network.

C. Microtubule asters

In cells, spindles are positioned for cell division by microtubule asters which emanate from the spindle poles and grow out towards the cortex; see Fig. 4 (C). In smaller cells, microtubules interacting with cortex are important for spindle positioning [33, 57, 58]. Recent work in *C. elegans* embryos suggests that dynein mediated pulling forces from cortically bound dynein are crucial [59].

In larger cells, such as the *Xenopus* zygote, the situation is somewhat more complicated, since cytoskeletal filaments are in general much shorter than the typical cell radii [60]. Thus it has been proposed that in these cells spindles are positioned by cytoplasmic pulling, that is by dynein motors which carry a cargo from the aster periphery towards its center. This would cause an active drag against the cytoplasmic fluid, which would ultimately cause spindle centering [61, 62]. To test this hypothesis the authors of [63] co-imaged the cytoskeletal actin, microtubules, and membranous networks. They find that these networks move against each other near aster boundaries, but move together near the asters center. It is thus tempting to ask what explains these different behaviors. One appealing hypothesis is that these asters are highly crosslinked near their centers, and less crosslinked near aster cores.

D. Artificial systems

Given the complexity and the sheer number of different constituents of cytoskeletal networks in living cells, biophysicists have developed simplified *in vitro* systems made from cytoskeletal components; see Fig. 4 (C). Here, the physics of cytoskeletal networks can be studied at a reduced complexity and in a more controllable environment. Beyond that, they have provided foundational examples of out-of-equilibrium materials.

One prominent system by [64] is made from stable microtubules and kinesin-1 motors joined by engineered linkers. This same mixture has been used to study active materials in bulk and on 2d interfaces [64], in vesicles [65], rigid confinements [66, 67] and droplets [68]. The same system has also been adapted to study disclination loops in 3d active nematics [69]. It is surprising, given the importance of these systems, that the structure and number of crosslinks that bind microtubules remain relatively unexplored. More studies will be needed to solidly classify these particular systems as either highly or sparsely crosslinked.

Somewhat more recently, actin-based active networks have been synthesized. Many of the key findings of this line of research are summarized in [70]. These systems are in general driven by the molecular motor myosin and require the admixture of passive crosslinkers to generate active contractions. This peculiarity has been attributed to a liquid-gel transition, which may imply that the contractile states of these actomyosin networks are in the highly crosslinked regime.

There is a growing list of *in vitro* systems, using different motors and filaments assembled in cell extract or fully reconstituted such as in [71, 72] or the ones reviewed in [70, 73]. For most of these systems it remains unclear where they fall on the range from sparsely to highly connected systems.

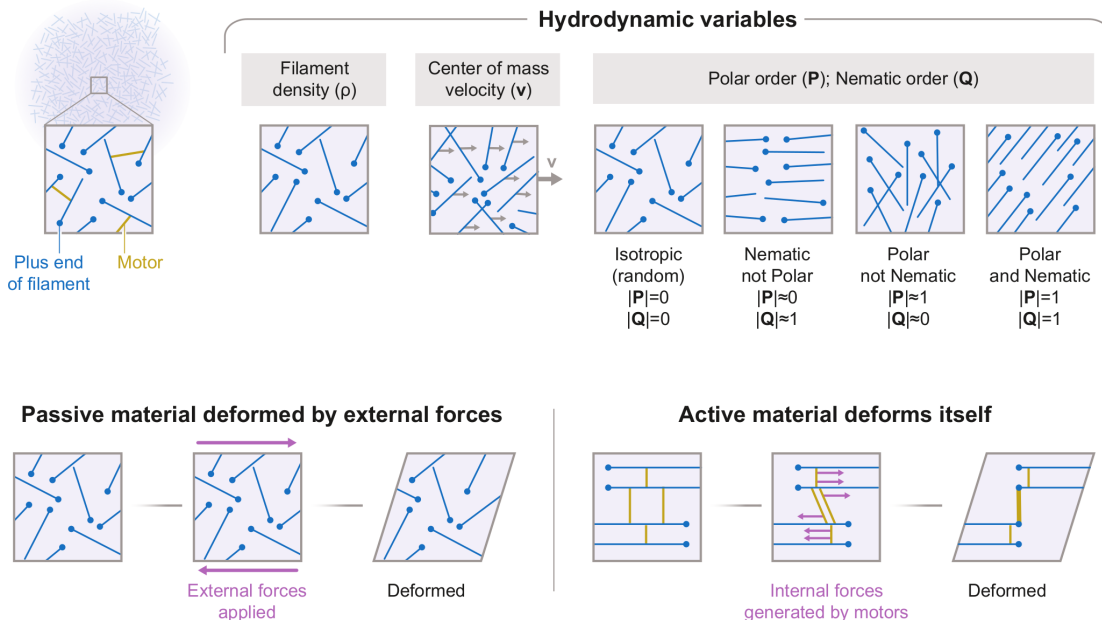


FIG. 5: Top: Illustration of the important hydrodynamic variables. Bottom: Illustration of externally strained and self-strained materials.

IV. THEORETICAL DESCRIPTIONS OF CYTOSKELETAL SYSTEMS

Much of our current theoretical understanding of cytoskeletal active matter derives from the remarkable success of extending the broken-symmetry hydrodynamics of liquid crystal system [9] to active materials where micro-scale non-equilibrium processes can generate force and torque dipoles [4–6]. These theories have clarified the fields (densities, velocities, order parameters) through which to describe the dynamics of a cytoskeletal material on long-wave hydrodynamic scales; see Fig. 5, and which material properties, such as the viscosities and activity coefficients, are needed to characterize these materials. More microscopic theories derive the values of material properties and their microscopic origins.

We start by reviewing the fields and material properties that we use to characterize cytoskeletal materials. We then review theoretical predictions for how these material properties are determined in highly and sparsely crosslinked networks.

A. Hydrodynamic variables

We seek to describe the evolution of a cytoskeletal system with a small number of continuous fields. At large length and time scales the fields needed to sufficiently characterize a material are those associated with conserved quantities and those associated to continuous broken symmetries [74]; see Fig. 5 (top). We first introduce the fields associated to conserved quantities.

The first is the total mass density $\rho^{\text{tot}}(\mathbf{x}, t)$ of the material. Since mass can be neither created nor destroyed,

$$\partial_t \rho^{\text{tot}} = -\nabla \cdot \mathbf{g}^{\text{tot}}, \quad (7)$$

where $\mathbf{g}^{\text{tot}}(\mathbf{x}, t)$, denotes the total mass flux - or momentum density. In the cytoskeletal systems of interest here the total mass density consists of solvent and gel contributions, such that $\rho^{\text{tot}} = \rho + \rho^s$, where ρ is the gel contribution, by which we mean the mass of filaments and proteins attached to filaments. In general, chemical processes, such as filament nucleation and polymerization, and the binding and unbinding of proteins, can convert solvent mass into gel mass and vice versa. Thus we can write

$$\partial_t \rho = -\nabla \cdot \rho \mathbf{v} + R \quad (8)$$

$$\partial_t \rho^s = -\nabla \cdot \rho^s \mathbf{v}^s - R, \quad (9)$$

where R is the mass conversion rate from chemical reactions and we have defined the gel and solvent velocities by $\mathbf{g}^{\text{tot}} = \rho\mathbf{v} + \rho^s\mathbf{v}^s$. In living materials the dominant contribution to R is filament polymerization and depolymerization, which in general is highly regulated. For instance in *Xenopus*'s meiotic spindles the dominant mode of filament creation is autocatalytic, and new filaments nucleate in a branching process from preexisting ones [47–53].

The second field that arises from conservation considerations is the momentum density itself. In the absence of external forces, the momentum density $\mathbf{g}^{\text{tot}}(\mathbf{x}, t)$ can only change by a momentum flux

$$\partial_t \mathbf{g}^{\text{tot}} = \nabla \cdot \boldsymbol{\Sigma}^{\text{tot}}, \quad (10)$$

where $\boldsymbol{\Sigma}^{\text{tot}}(\mathbf{x}, t)$ is total stress in the material. Like the mass flux we can write $\boldsymbol{\Sigma}^{\text{tot}} = \boldsymbol{\Sigma} + \boldsymbol{\Sigma}^s$, and force balance equations for the gel and solvent components of the material separately. Under the assumptions that the solvent is Newtonian, that inertial terms can be neglected, and that the force exerted between the gel and fluid phases is linear in the gel density and their velocity difference, one recovers Eqns. (3,4). Thus, the fields that we need to keep track of, since they are associated to conserved quantities, are ρ, ρ^s, \mathbf{v} , and \mathbf{v}^s . We next introduce the fields that are associated with continuous broken symmetries.

Order parameter fields characterize the conformational state of the material. For the purposes here we assume that cytoskeletal filaments are rod-like and rigid. Then the tensor orientation order parameter $\mathcal{Q}(\mathbf{x}, t)$ naturally arises. From \mathcal{Q} devolves the scalar orientation order parameter and director field. Unlike purely nematic systems, cytoskeletal filaments like microtubules or actin are polar, as are the motor-mediated forces acting upon them. Hence, we will also need a polar order parameter $\mathbf{P}(\mathbf{x}, t)$. If the system were characterized at the microscopic level by a particle distribution function $\psi(\mathbf{x}, \mathbf{p}, t)$ [8] with \mathbf{p} being the particle orientation vector on the 2-sphere, then these order parameters arise as its \mathbf{p} -moments $\mathbf{P} = \langle \mathbf{p} \rangle / \rho$ and $\mathcal{Q} = \langle \mathbf{p}\mathbf{p} \rangle / \rho$, where the angular brackets denote a distributional averaging over the \mathbf{p} -sphere. In general higher order symmetry fields exist, but we ignore them here for simplicity.

In summary, we seek to describe the cytoskeletal systems in terms of just a few coarse grained continuous fields. They are the densities ρ and ρ^s , the velocity fields \mathbf{v} and \mathbf{v}^s , and the order parameter fields \mathcal{Q} and \mathbf{P} . Thus, the next task is to arrive at expression for the stresses $\boldsymbol{\Sigma}^{\text{tot}}$ and $\boldsymbol{\Sigma}$, and the transport operators for the order parameter fields \mathcal{Q} and \mathbf{P} , and the chemical reaction rate R , in terms of hydrodynamic variables. In this review we are concerned with the expressions for the stresses first and foremost.

B. Material properties of active cytoskeletal networks

Given the set of hydrodynamic variables, symmetry-based theories postulate material laws for all unknown quantities by writing down all symmetry allowed terms that respect the invariances of the systems, such as translation and rotation invariance. How to obtain symmetry based material equations from symmetry considerations or from non-equilibrium thermodynamics considerations is reviewed elsewhere in great detail [6, 21].

For our purposes here, it is sufficient to express the total stress by the equation,

$$\boldsymbol{\Sigma}^{\text{tot}} = \chi^v : \nabla \mathbf{v} + \chi^s : \nabla \mathbf{v}^s + \chi^a : \nabla \mathbf{P} + \Pi^a \mathcal{I} + \mathcal{A}^{(\mathbf{P})} \mathbf{P} \mathbf{P} - \mathcal{A}^{(\mathcal{Q})} \mathcal{Q} + \bar{\boldsymbol{\Sigma}}, \quad (11)$$

which obeys the symmetry constraints discussed in [6, 21]. Here, χ^v is the fourth-rank gel viscosity tensor, χ^s is a fourth-rank solvent viscosity tensor, and χ^a is a fourth-rank tensor that quantifies active polar stresses proportional to gradients in gel polarity \mathbf{P} . The coefficients $\mathcal{A}^{(\mathbf{P})}$ and $\mathcal{A}^{(\mathcal{Q})}$ quantify the magnitude of active polar and active nematic stresses in the material, respectively. Furthermore Π^a acts as an active pressure and $\bar{\boldsymbol{\Sigma}}$ denotes other stresses in the system, which stem from hydrostatic and steric exclusion and alignment effects. For an in-depth discussion see [9] and [6]. Together, $\chi^v, \chi^a, \chi^s, \Pi^a, \mathcal{A}^{(\mathbf{P})}$, and $\mathcal{A}^{(\mathcal{Q})}$ are the material properties of the cytoskeletal filament network. They in turn depend on the state of the network, that is the hydrodynamic variables, and need either be measured in an experiment, or derived from more microscopic considerations to allow a complete description of the material. Symmetry-based theories also elucidate the form of the transport equations for \mathbf{P} and \mathcal{Q} . We refer to [6, 21] for a more complete discussion.

In this review we are concerned with theories that derive expressions for the phenomenological coefficients in (Eq. (11)) from micro-scale considerations of motors and filaments. In particular we want to contrast theories for highly crosslinked and sparsely crosslinked systems. We will highlight that the functional dependencies of $\chi^v, \chi^a, \chi^s, \Pi^a, \mathcal{A}^{(\mathbf{P})}$ and $\mathcal{A}^{(\mathcal{Q})}$ change between these two regimes.

C. The highly crosslinked regime of cytoskeletal networks

We first review theories for the hydrodynamic limit of the highly crosslinked regime of cytoskeletal networks. We consider a cytoskeletal material to be highly crosslinked if $\ell^g \gg \ell^s$. The hydrodynamic limit of such a material is

dominated by crosslink interactions, and thus solvent mediated interactions can be ignored, since the length scale of momentum transport associated with Σ is much larger than that associated with Σ^s ; see Fig. 3. Thus these theories assume that $\Sigma^{\text{tot}} = \Sigma$ which implies $\mathbf{v}^s = \mathbf{v}$ and that Σ^s is negligible.

To our knowledge this limit of active gels was first discussed in the context of studying actin bundles [19, 75] where the authors proposed a 1d model for describing actin structures in the cortex. Only recently have these ideas been extended to larger three-dimensional systems. In [14, 20] a phenomenological model for the force density \mathbf{f}_{ij} , generated by crosslinks between filaments, was proposed. In this model the force density is given by

$$\begin{aligned} \mathbf{f}_{ij} = & K(s_i, s_j) (\mathbf{x}_i + s_i \mathbf{p}_i - \mathbf{x}_j - s_j \mathbf{p}_j) \\ & + \gamma(s_i, s_j) (\mathbf{v}_i + s_i \dot{\mathbf{p}}_i - \mathbf{v}_j - s_j \dot{\mathbf{p}}_j) \\ & + [\sigma(s_i, s_j) \mathbf{p}_i - \sigma(s_j, s_i) \mathbf{p}_j]. \end{aligned} \quad (12)$$

The functions $K(s_i, s_j)$, $\gamma(s_i, s_j)$, $\sigma(s_i, s_j)$ characterize the types of forces exerted by crosslink populations between the arclength positions s_i, s_j on filaments i , and j . The coefficient K captures effects of crosslink elasticity, the coefficient γ acts as an effective frictional coupling between filaments, and σ characterizes the active forcing from motor stepping; see Fig. 2. The main conceptual advance between this phenomenological model and the ones proposed in earlier work, is that here \mathbf{f}_{ij} explicitly depends on the velocities and rates of rotation of filaments i, j . With this dependence, in a dense system the dynamics of all filaments in the system becomes tightly coupled. In contrast, earlier work [11, 18, 23, 76] had posited motor interactions that depend only on the relative orientations and center of mass positions of filaments, effectively constraining themselves to pairwise interactions.

From Eq. (12) one calculates the stress in the network using

$$\Sigma = -\frac{1}{2} \sum_{i,j} \left[\frac{\delta(\mathbf{x} - \mathbf{x}_i) \delta(\mathbf{x}' - \mathbf{x}_j)}{(\mathbf{x}_i - \mathbf{x}_j + s_i \mathbf{p}_i - s_j \mathbf{p}_j) \mathbf{f}_{ij}} \right]_{\Omega(\mathbf{x}_i)}^{ij} \quad (13)$$

where the brackets $[\dots]_{\Omega(\mathbf{x}_i)}^{ij}$ denotes the coarse graining operation

$$[\phi]_{\Omega(\mathbf{x}_i)}^{ij} = \int_{-\frac{L}{2}}^{\frac{L}{2}} ds_i \int_{-\frac{L}{2}}^{\frac{L}{2}} ds_j \int_{\Omega(\mathbf{x}_i)} d\mathbf{x}^3 \phi. \quad (14)$$

Here $\Omega(\mathbf{x})$ is a sphere centered around the point \mathbf{x} and whose radius R is the size (maximal extension) of the cross-linker. In this version of the theory, all filaments are taken to have the same length L . Thus, the operation $[\dots]_{\Omega(\mathbf{x}_i + s_i \mathbf{p}_i)}^{ij}$ integrates its argument over all geometrically possible crosslink induced interactions.

The emergent material properties turn out to depend on a small set of s -moments of the phenomenological coefficients K , γ , σ . These moments are given by

$$X_{nm}(\mathbf{x}) = [X(s_i, s_j) s_i^n s_j^m]_{\Omega(\mathbf{x})}^{ij}, \quad (15)$$

where X can be K , γ , or σ . More explicitly,

$$K_0 = K_{00} = [K(s_i, s_j)]_{\Omega(\mathbf{x}_i)}^{ij}, \quad (16)$$

$$K_1 = K_{10} = K_{01} = [s_i K(s_i, s_j)]_{\Omega(\mathbf{x}_i)}^{ij}, \quad (17)$$

$$\gamma_0 = \gamma_{00} = [\gamma(s_i, s_j)]_{\Omega(\mathbf{x}_i)}^{ij}, \quad (18)$$

$$\gamma_1 = \gamma_{10} = \gamma_{01} = [s_i \gamma(s_i, s_j)]_{\Omega(\mathbf{x}_i)}^{ij}, \quad (19)$$

$$\sigma_0 = \sigma_{00} = [\sigma(s_i, s_j)]_{\Omega(\mathbf{x}_i)}^{ij}, \quad (20)$$

$$\sigma_{10} = [s_i \sigma(s_i, s_j)]_{\Omega(\mathbf{x}_i)}^{ij}, \quad (21)$$

$$\sigma_{01} = [s_j \sigma(s_i, s_j)]_{\Omega(\mathbf{x}_i)}^{ij}. \quad (22)$$

With these definitions, one finds for the viscosity tensor

$$\chi_{\alpha\beta\gamma\mu}^{\nu} = \rho^2 \gamma_0 \left(\frac{3R^2}{10} \delta_{\alpha\gamma} \delta_{\beta\mu} + \frac{L^2}{12} \gamma_0 (Q_{\alpha\gamma} \delta_{\beta\mu} - Q_{\alpha\beta} Q_{\gamma\mu}) \right), \quad (23)$$

and, very importantly, that

$$\chi_{\alpha\beta\gamma\mu}^a = \frac{\sigma_0}{\gamma_0} \chi_{\alpha\beta\gamma\mu}^v. \quad (24)$$

for the coefficient quantifying the active polar stress.

The relation between Eqs. (23) and (24) implies that we can combine the first two terms of Eq. 11 into

$$\Sigma^{ss} = \chi^v : \left(\nabla \mathbf{v} + \frac{\sigma_0}{\gamma_0} \nabla \mathbf{P} \right) \quad (25)$$

which we call the self-straining stress. In this type of material σ_0/γ_0 is essentially the free velocity of the motors and crosslinks coupling filaments. Thus the state of zero self-straining stress is one where the viscous stress exactly balances the active polar stress, which can be achieved when all filaments in the material move at the motor speed in the direction in which they point [14]. This self-straining state is a consequence of the fact that the same active crosslinks which drive filament motion also couple the dynamics over long length scales. In essence, in a material where the crosslinking is provided by active crosslinks, filaments can move through the material at the preferred speed of the motor without stressing the material; see Fig. 5.

The same calculation also makes predictions for other active stresses in the material [20]. One finds

$$A^{(\mathcal{Q})} = \rho^2 (\sigma_{10} - \sigma_0 \frac{\gamma_1}{\gamma_0} + \frac{L^2}{12} K_0), \quad (26)$$

$$A^{(\mathbf{P})} = \rho^2 (\sigma_{01} - \sigma_0 \frac{\gamma_1}{\gamma_0}), \quad (27)$$

$$\Pi^a = \rho^2 \frac{3R^2}{10} K_0. \quad (28)$$

These expressions generalize to the continuum limit the predictions made by [77] in the context of a discrete model.

An analogous calculation provides expressions for the filament speed \mathbf{v}_i and rotation rate $\dot{\mathbf{p}}_i$ in the lab frame:

$$\mathbf{v}_i - \mathbf{v} = \frac{\sigma_0}{\gamma_0} (\mathbf{p}_i - \mathbf{P}) + \mathcal{O}(L^2) \quad (29)$$

and

$$\dot{\mathbf{p}}_i = (\mathcal{I} - \mathbf{p}_i \mathbf{p}_i) \cdot \left\{ \begin{array}{l} (\nabla \mathbf{v} + \frac{\sigma_0}{\gamma_0} \nabla \mathbf{P}) \cdot \mathbf{p}_i \\ + \frac{12}{\gamma_0 L^2 \rho^2} \mathcal{E} \cdot \mathbf{p}_i \\ + \frac{12}{\gamma_0 L^2} A^{(\mathbf{P})} \mathbf{P} \end{array} \right\}, \quad (30)$$

where \mathcal{E} is the steric distortion field [9]. We refer the reader to [20] for additional detail.

D. The sparsely crosslinked regime of cytoskeletal networks

We now review theories of the sparsely crosslinked regime of cytoskeletal networks. We consider a cytoskeletal material to be sparsely crosslinked if $\ell^s \gg \ell^g$, so that the hydrodynamic (long-wave) limit is dominated by fluid mediated interactions and the viscous transport of momentum though the gel is negligible; see Fig. 3. Thus, these approaches proceed from Eq. (4). Given a microscopic model of how the gel deforms in the fluid, these models proceed to calculate the active stresses Σ^a , typically reflecting force dipoles acting on the solvent. Thus, $\Gamma\rho(\mathbf{v} - \mathbf{v}^s) \simeq \nabla \cdot \Sigma^a$. This implies $\Sigma^{\text{tot}} = \Sigma^s + \Sigma^a$. The motion of the gel generally takes the form $\mathbf{v}^s - \mathbf{v} \propto \mathbf{P}$, which allows polar pieces of gel to 'swim' through the solvent.

One such line of models devolves from the mechanics of swimming suspensions. To study the dynamics of suspensions of hydrodynamically interacting swimming microorganisms, Saintillan & Shelley [78, 79] developed a kinetic theory coupling a Smoluchowski equation for particle position and orientation to a forced Stokes equation; see also [22, 80, 81]. At the particle level, free swimmers (which are force dipoles in the solvent) are treated as rod-like particles swimming in a locally linear flow, propelled by a prescribed active surface stress. The swimmer velocity, rotation rate, and entire surface stress, can be calculated in terms of the background flow, with the background flow itself determined through solution of a forced Stokes equation. The forcing is through an "extra stress" found using Batchelor's adaptation [82], for dilute suspensions, of Kirkwood theory. In its simplest formulation, Saintillan & Shelley find the coupled Smoluchowski equation for the particle distribution function $\psi(\mathbf{x}, \mathbf{p}, t)$

$$\partial_t \psi + \nabla_x \cdot (\dot{\mathbf{x}} \psi) + \nabla_p \cdot (\dot{\mathbf{p}} \psi) = 0, \quad \text{where } \dot{\mathbf{x}} = \mathbf{v}^s(\mathbf{x}) + U_0 \mathbf{p} \text{ and } \dot{\mathbf{p}} = (\mathbf{I} - \mathbf{p} \mathbf{p}) \nabla \mathbf{v}^s(\mathbf{x}) \mathbf{p}, \quad (31)$$

where \mathbf{p} is swimmer orientation and U_0 is its undisturbed speed, and the last expression is Jeffrey's equation (cf. Eq. (29,30)). The solvent velocity \mathbf{v}^s is found through solution of a Stokes equation driven by an active dipolar stress Σ^a :

$$-\nabla_x \Pi^s + \mu \Delta \mathbf{v}^s = -\nabla_x \cdot \Sigma^a \text{ and } \nabla_x \cdot \mathbf{v}^s = 0, \text{ with } \Sigma^a = \alpha_0 \rho \mathcal{Q}. \quad (32)$$

Here, α_0 is the so-called dipole strength whose sign reflects whether the swimmer force dipole is extensile ($\alpha_0 < 0$) or contractile ($\alpha_0 > 0$). This categorization depends upon the detailed placement of thrust and no-slip regions on the effective swimmer body. This theory predicts both the instability of aligned suspensions [83, 84], and the instability of isotropic extensile suspensions when swimmers exceed a critical concentration [79, 84, 85]. In later work [84], inter-particle aligning torques and consequent stresses, based on Maier-Saupe theory [8], were introduced to capture sterically-induced concentration effects; see [86] for a review.

Gao *et al.* [12, 87] adapted this approach to treating immersed assemblies of microtubules undergoing polarity sorting by multimeric motor complexes such as the engineered kinesin-1 complexes used in [64]. To do this, as the basic unit they considered nematically ordered local clusters of microtubules, say with n of them pointing rightwards and m pointing leftwards (hence, $\mathbf{P} = (n - m)/(n + m)\hat{\mathbf{x}}$); see Figure 1 of [12]. It is assumed that every microtubule pair in the cluster is connected by active, plus-end directed cross-linkers moving at speed v_w on each microtubule. The coupling between the anti-aligned populations induces a minus-end directed relative sliding for each. By using Stokesian slender-body theory [88] and assuming that the solvent drag thus calculated is the only force resisting microtubule motion they calculated the velocities of the left- and rightward pointing MTs to be $v_L = (2n/n + m)v_w$ and $v_R = -(2m/n + m)v_w$. This yields $v_R - v_L = -2v_w$. Slender-body theory again yields the forces each rod exerts upon the fluid, and hence the induced "extra stress" tensor arising from polarity sorting within the bundle can be calculated and is found to be proportional to $v_w mn/(m + n)\hat{\mathbf{x}}\hat{\mathbf{x}}$.

Thus, in a cluster with $m = n$, the two populations are pulled past each other with equal speed v_w , while producing a maximal polarity-sorting stress. If most microtubules point rightwards, so that $m \approx 0$, then $v_L \approx 2v_w$ and $v_r \approx 0$, and the polarity sorting extra stress is small (with a like statement if $n \approx 0$). That the microtubule speeds depends upon the polarity is a consequence of the micro-mechanical model wherein only solvent drag resists microtubule translocation.

Adapting this cluster picture to a more general setting where the cluster also moves with the background fluid velocity, Gao *et al.* give the analogous result to Eqs. (31,32) where the microtubule flux and active stress tensor, induced by polarity sorting of anti-aligned microtubules (aa), are given by

$$\dot{\mathbf{x}} = \mathbf{v}^s(\mathbf{x}) + v_w(\mathbf{P} - \mathbf{p}), \text{ and } \Sigma^{aa} = \alpha_{aa}\rho(\mathcal{Q} - \mathbf{P}\mathbf{P}). \quad (33)$$

These forms for $\dot{\mathbf{x}}$ and Σ^{aa} reproduce exactly the nematic cluster results above, and show the dependence polarity sorting of the microtubule velocity upon the local polarity $\mathbf{P}(\mathbf{x})$.

This theory was further informed by detailed Brownian/Monte-Carlo simulations of nematic assemblies of rigid filaments interacting through multimeric kinesin-1 motors, thermal noise, and steric interactions. From these simulations were gleaned estimates of the activity coefficient α_{aa} giving that $\alpha_{aa} < 0$, i.e. that polarity sorting dipolar stresses were extensile [12, 87]. The stochastic simulations also showed the presence of an additional subdominant, active and extensile stress, having the form $\alpha_{pa}\rho(\mathcal{Q} + \mathbf{P}\mathbf{P})$, arising from the relaxation of cross-link tethers of multimeric motors connecting polar-aligned (pa) microtubules [89]. With this continuum model in hand, they analyzed and simulated the dynamics of a thin layer of active material at the interface between two fluids. Their analysis demonstrated the existence of a characteristic finite length-scale of instability due to the external drag of the outer fluids, and of orientational instabilities for aligned states. Their simulations of the full kinetic theory showed a nonlinear dynamics of fluid and material flows, and of nucleating/annihilating disclination defect pairs, with a structure qualitatively similar to that observed experimentally in [64].

To make comparisons to the highly cross-linked regime, the total stress in the Gao *et al.* model has the form

$$\Sigma^{tot} = \Sigma^s + \Sigma^a = -\Pi^s \mathcal{I} + \mu (\nabla \mathbf{v}^s + \nabla \mathbf{v}^s{}^T) + (\alpha_{pa} + \alpha_{aa})\rho \mathcal{Q} + (\alpha_{pa} - \alpha_{aa})\rho \mathbf{P}\mathbf{P} + \tilde{\Sigma}^s. \quad (34)$$

where $\tilde{\Sigma}^s$ contains stresses arising from steric interactions (from Maier-Saupe theory) and particle rigidity; compare to Eq. (11). Here, the microtubule flux in Eq. (33) is of the same form as in the highly cross-linked case but with the solvent velocity rather than the material velocity \mathbf{v} [14]; compare Eq. (29). Unlike the stress in the highly crosslinked regime, the expression in Eq. (34) does not depend upon $\nabla \mathbf{P}$. It is the relation between $\nabla \mathbf{P}$ and $\nabla \mathbf{v}$ revealed by Eq. (24) that underlays the self-straining state of the highly cross-linked state; see Fig. 5.

The cluster picture in [12] can be generalized by allowing 'cluster-cluster' interactions which can lead to additional stresses proportional to gradient in the local polarity. Efforts along these lines were first made in [76, 90]. There the key assumption is that pairs of filaments interact via sparse coupling of constant velocity motors. This theory also provided an initial understanding of the origin of contractile behaviors found in many early experiments of filament/motor mixtures.

V. SYNTHESIS AND OPEN CHALLENGES

Cytoskeletal networks are the drivers of basic biological functions like cell division and cell motility. The constituents of cytoskeletal networks also provide foundational examples in the field of active matter. In this review we highlight the differences between the physics of highly crosslinked and sparsely crosslinked cytoskeletal networks. In highly crosslinked systems the long-ranged transport of momentum is mediated through the crosslinks themselves ($\ell^g \gg \ell^s$), whereas in sparsely crosslinked systems it is the solvent that plays that role ($\ell^s \gg \ell^g$); see Fig. 3

This has important implications for the resulting material properties. In highly crosslinked materials, the same crosslinkers which generate the driving forces between filaments also generate the frictional coupling that keeps the networks coherent. Consequently, active stresses and the viscosity of the material are intimately linked. In particular, the polar active stress proportional to polarity gradients is linked to the viscosity tensor by Eq. (??). For these materials, the viscous and polar stresses exactly balance when all filaments in the material move at the preferred motor velocity σ_0/γ_0 in the direction to which they point [14]. Since χ^v and χ^a vary together the properties of this state are not sensitive to protein concentrations. This self-straining state is not just a theoretical curiosity; it has been observed *in vitro* [14] and in spindles [17, 91].

In contrast, in the sparsely crosslinked regime the viscosity tensor χ^v of the material is largely set by the viscosity of the solvent in which filaments are suspended and is thus independent of concentrations and properties of the crosslinking molecules, while the values of active stresses depend on protein concentrations. This provides a possible diagnostic for differentiating highly crosslinked and sparsely crosslinked active materials by modulating crosslink concentrations. Moreover, in the self-straining state of active materials filaments can move through the material at speeds that are independent of the local polar and nematic order [14], whereas in more sparsely crosslinked systems [12] the motion of filaments throughout the system depends on the local polarity.

A second striking difference between the highly crosslinked and sparsely crosslinked materials is the form of the other active stresses $\mathcal{A}^{(Q)}$, $\mathcal{A}^{(P)}$. It has long been known that contractile (or extensile) stresses can be generated only if motors act in a way that breaks the symmetry between extending and contracting single filament pairs. This could for instance be achieved by end-clustering or end-binding affinities of motor proteins [18, 90]. On top of that, the mathematics of the highly crosslinked regime requires that $\sigma_1 \neq \gamma_1/\gamma_0\sigma_0$; see Eqns. (26,27). This means that the anisotropy of friction (γ_1/γ_0) along filaments needs to be different from the anisotropy of motor drive (σ_1/σ_0) to generate active contractions. In practice this can be achieved by either mixing several types of crosslinks or by creating a crosslink with two different motor heads [20]. This prediction might shed insight into the well known - but so far poorly understood - observation that in many actomyosin systems contractions only occur if a small amount of passive crosslinker is added to the system [92].

A third important difference between the highly and sparsely crosslinked regimes comes from the fact that the solvent is incompressible, while the network itself can be compacted by active processes. As a consequence sparsely crosslinked theories predict incompressible material flow fields, while highly crosslinked theories can predict active bulk contraction. Thus it is tempting to speculate that contractile systems like [71, 72] are highly crosslinked. In contrast many classic active nematic experiments show no clear signs of compaction [35, 64, 67].

In section III we sought to classify biological and experimental active matter systems as being either highly or sparsely crosslinked. We believe that many important systems, such as the cell cortex and many spindles, are highly crosslinked. For most systems however, this assertion remains an educated guess rather than an experimental certainty. Given the increasing awareness that the physics of active cytoskeletal networks can be drastically different for different numbers of crosslinks, we hope that this review will serve to highlight the need for experiments that will answer this question more definitively.

Finally, we want to conclude by remarking that many active systems are likely to live in the intermediate regime between highly and sparsely crosslinked. One example are the microtubule asters studied in extract [63], which are probably highly crosslinked in their bulk, but more sparsely crosslinked near their boundaries. These structures are biologically important and revelatory of new physics in an intermediate crosslinking regime that is so far barely explored.

In summary, we firmly believe that the science of biologically active materials will benefit greatly by simply enumerating the number of crosslinks active in the materials of interest. This enumeration will help identify important and distinct physical regimes, and help make theories quantitative and living systems engineerable.

Acknowledgements: We thank James Pelletier, Steffanie Redemann, and Kun-Ta Wu for providing us with experimental images. We thank Lucy Reading-Ikkanda for preparation of figures. MJS acknowledges support from NSF grants DMR-2004469 and DMR-1420073 (NYU-MRSEC). We thank our many collaborators who worked with

us in this area.

-
- [1] J. Howard. *Mechanics of motor proteins and the cytoskeleton*. Sinauer Associates, Publishers, 2001.
- [2] B. Alberts, A. Johnson, J. Lewis, , Roberts K., and P. Walter. *Molecular Biology of the Cell 5th edition*. Garland Science, New York, 2007.
- [3] Peter J Foster, Sebastian Fürthauer, Michael J Shelley, and Daniel J Needleman. From cytoskeletal assemblies to living materials. *Current opinion in cell biology*, 56:109–114, 2019.
- [4] Karsten Kruse, Jean-Francois Joanny, Frank Jülicher, Jacques Prost, and Ken Sekimoto. Generic theory of active polar gels: a paradigm for cytoskeletal dynamics. *The European Physical Journal E*, 16(1):5–16, 2005.
- [5] S Fürthauer, M Stempel, SW Grill, and F Jülicher. Active chiral fluids. *The European physical journal. E, Soft matter*, 35:89, 2012.
- [6] Frank Jülicher, Stephan W Grill, and Guillaume Salbreux. Hydrodynamic theory of active matter. *Reports on Progress in Physics*, 81(7), 2018.
- [7] Sundar Ram Naganathan, Sebastian Fürthauer, J. Rodriguez, B. T. Fievet, Frank Jülicher, J. Ahringer, C. V. Cannistraci, and S.W. Grill. Morphogenetic degeneracies in the actomyosin cortex. *Elife*, 7:e37677, 2018.
- [8] Masao Doi, Samuel Frederick Edwards, and Samuel Frederick Edwards. *The theory of polymer dynamics*, volume 73. oxford university press, 1988.
- [9] P. G. de Gennes and J. Prost. *The physics of liquid crystals*. Clarendon Press, 1995.
- [10] Tanniemola B Liverpool and M Cristina Marchetti. Instabilities of isotropic solutions of active polar filaments. *Physical Review Letters*, 90(13):138102, 2003.
- [11] Igor S Aranson and Lev S Tsimring. Pattern formation of microtubules and motors: Inelastic interaction of polar rods. *Physical Review E*, 71(5):050901, 2005.
- [12] Tong Gao, Robert Blackwell, Matthew A. Glaser, M. D. Betterton, and Michael J. Shelley. Multiscale polar theory of microtubule and motor-protein assemblies. *Phys. Rev. Lett.*, 114:048101, Jan 2015.
- [13] Chase P Broedersz and Fred C MacKintosh. Modeling semiflexible polymer networks. *Reviews of Modern Physics*, 86(3):995, 2014.
- [14] Sebastian Fürthauer, Bezia Lemma, Peter J Foster, Stephanie C Ems-McClung, Che-Hang Yu, Claire E Walczak, Zvonimir Dogic, Daniel J Needleman, and Michael J Shelley. Self-straining of actively crosslinked microtubule networks. *Nature Physics*, pages 1–6, 2019.
- [15] TJ Mitchison. Polewards microtubule flux in the mitotic spindle: evidence from photoactivation of fluorescence. *The Journal of cell biology*, 109(2):637–652, 1989.
- [16] Ge Yang, Lisa A Cameron, Paul S Maddox, Edward D Salmon, and Gaudenz Danuser. Regional variation of microtubule flux reveals microtubule organization in the metaphase meiotic spindle. *The Journal of cell biology*, 182(4):631–639, 2008.
- [17] Benjamin A Dalton, David Oriola, Franziska Decker, Frank Jülicher, and Jan Brugués. A gelation transition enables the self-organization of bipolar metaphase spindles. *bioRxiv*, 2021.
- [18] Karsten Kruse and F Jülicher. Actively contracting bundles of polar filaments. *Physical Review Letters*, 85(8):1778, 2000.
- [19] Karsten Kruse and Frank Jülicher. Self-organization and mechanical properties of active filament bundles. *Physical Review E*, 67(5):051913, 2003.
- [20] Sebastian Fürthauer, Daniel J Needleman, and Michael J Shelley. A design framework for actively crosslinked filament networks. *New Journal of Physics*, 23(1):013012, 2021.
- [21] MC Marchetti, JF Joanny, S Ramaswamy, TB Liverpool, J Prost, Madan Rao, and R Aditi Simha. Hydrodynamics of soft active matter. *Reviews of Modern Physics*, 85(3):1143, 2013.
- [22] David Saintillan and Michael J Shelley. Active suspensions and their nonlinear models. *Comptes Rendus Physique*, 14(6):497–517, 2013.
- [23] Ivan Maryshev, Davide Marenduzzo, Andrew B Goryachev, and Alexander Morozov. Kinetic theory of pattern formation in mixtures of microtubules and molecular motors. *Physical Review E*, 97(2):022412, 2018.
- [24] Marcel E Janson, Rose Loughlin, Isabelle Loïdice, Chuanhai Fu, Damian Brunner, François J Nédélec, and Phong T Tran. Crosslinkers and motors organize dynamic microtubules to form stable bipolar arrays in fission yeast. *Cell*, 128(2):357–368, 2007.
- [25] D. Head, W. Briels, and G. Gompper. Nonequilibrium structure and dynamics in a microscopic model of thin-film active gels. *Phys. Rev. E*, 89:032705, 2014.
- [26] Konstantin Popov, James Komianos, and Garegin A. Papoian. MEDYAN: Mechanochemical Simulations of Contraction and Polarity Alignment in Actomyosin Networks. *PLOS Computational Biology*, 12(4):e1004877, April 2016.
- [27] Simon L. Freedman, Shiladitya Banerjee, Glen M. Hocky, and Aaron R. Dinner. A Versatile Framework for Simulating the Dynamic Mechanical Structure of Cytoskeletal Networks. *Biophysical Journal*, 113(2):448–460, July 2017.
- [28] Claudio Collinet and Thomas Lecuit. Programmed and self-organized flow of information during morphogenesis. *Nature Reviews Molecular Cell Biology*, pages 1–21, 2021.
- [29] Stefanie Redemann, Johannes Baumgart, Norbert Lindow, Michael Shelley, Ehssan Nazockdast, Andrea Kratz, Steffen Prohaska, Jan Brugués, Sebastian Fürthauer, and Thomas Müller-Reichert. *C. elegans* chromosomes connect to centrosomes by anchoring into the spindle network. *Nature Communications*, 8:15288, May 2017. Article.

- [30] Thomas D Pollard. Actin and actin-binding proteins. *Cold Spring Harbor perspectives in biology*, 8(8):a018226, 2016.
- [31] Ray Alfaró-Aco and Sabine Petry. Building the microtubule cytoskeleton piece by piece. *Journal of Biological Chemistry*, 290(28):17154–17162, 2015.
- [32] Katherine Luby-Phelps. Cytoarchitecture and physical properties of cytoplasm: volume, viscosity, diffusion, intracellular surface area. *International review of cytology*, 192:189–221, 1999.
- [33] Carlos Garzon-Coral, Horatiu A Fantana, and Jonathon Howard. A force-generating machinery maintains the spindle at the cell center during mitosis. *Science*, 352(6289):1124–1127, 2016.
- [34] Dong Li, Lin Shao, Bi-Chang Chen, Xi Zhang, Mingshu Zhang, Brian Moses, Daniel E Milkie, Jordan R Beach, John A Hammer, Mithun Pasham, et al. Extended-resolution structured illumination imaging of endocytic and cytoskeletal dynamics. *Science*, 349(6251), 2015.
- [35] Kun-Ta Wu, Jean Bernard Hishamunda, Daniel TN Chen, Stephen J DeCamp, Ya-Wen Chang, Alberto Fernández-Nieves, Seth Fraden, and Zvonimir Dogic. Transition from turbulent to coherent flows in confined three-dimensional active fluids. *Science*, 355(6331), 2017.
- [36] Guillaume Salbreux, Guillaume Charras, and Ewa Paluch. Actin cortex mechanics and cellular morphogenesis. *Trends in cell biology*, 22(10):536–545, 2012.
- [37] Mirjam Mayer, Martin Depken, Justin S Bois, Frank Jülicher, and Stephan W Grill. Anisotropies in cortical tension reveal the physical basis of polarizing cortical flows. *Nature*, 467(7315):617–621, 2010.
- [38] Peter Gross, K Vijay Kumar, Nathan W Goehring, Justin S Bois, Carsten Hoegel, Frank Jülicher, and Stephan W Grill. Guiding self-organized pattern formation in cell polarity establishment. *Nature physics*, 15(3):293–300, 2019.
- [39] AC Callan-Jones, Verena Ruprecht, Stefan Wieser, Carl-Philipp Heisenberg, and Raphaël Voituriez. Cortical flow-driven shapes of nonadherent cells. *Physical review letters*, 116(2):028102, 2016.
- [40] Hervé Turlier, Basile Audoly, Jacques Prost, and Jean-François Joanny. Furrow constriction in animal cell cytokinesis. *Biophysical journal*, 106(1):114–123, 2014.
- [41] Priyamvada Chugh, Andrew G Clark, Matthew B Smith, Davide AD Cassani, Kai Dierkes, Anan Ragab, Philippe P Roux, Guillaume Charras, Guillaume Salbreux, and Ewa K Paluch. Actin cortex architecture regulates cell surface tension. *Nature cell biology*, 19(6):689–697, 2017.
- [42] Sundar Ram Naganathan, Sebastian Fürthauer, Masatoshi Nishikawa, Frank Jülicher, and Stephan W Grill. Active torque generation by the actomyosin cell cortex drives left–right symmetry breaking. *Elife*, 3:e04165, 2014.
- [43] Marco Fritzsche, Christoph Erenkämper, Emad Moendarbary, Guillaume Charras, and Karsten Kruse. Actin kinetics shapes cortical network structure and mechanics. *Science advances*, 2(4):e1501337, 2016.
- [44] Jian-Qiu Wu and Thomas D Pollard. Counting cytokinesis proteins globally and locally in fission yeast. *Science*, 310(5746):310–314, 2005.
- [45] Jan Brugués, Valeria Nuzzo, Eric Mazur, and Daniel J Needleman. Nucleation and transport organize microtubules in metaphase spindles. *Cell*, 149(3):554–564, 2012.
- [46] Jan Brugués and Daniel Needleman. Physical basis of spindle self-organization. *Proceedings of the National Academy of Sciences*, 111(52):18496–18500, 2014.
- [47] Sabine Petry, Céline Pugieux, François J Nédélec, and Ronald D Vale. Augmin promotes meiotic spindle formation and bipolarity in xenopus egg extracts. *Proceedings of the National Academy of Sciences*, 108(35):14473–14478, 2011.
- [48] Sabine Petry, Aaron C Groen, Keisuke Ishihara, Timothy J Mitchison, and Ronald D Vale. Branching microtubule nucleation in xenopus egg extracts mediated by augmin and tpx2. *Cell*, 152(4):768–777, 2013.
- [49] Doogie Oh, Che-Hang Yu, and Daniel J Needleman. Spatial organization of the ran pathway by microtubules in mitosis. *Proceedings of the National Academy of Sciences*, 113(31):8729–8734, 2016.
- [50] Bryan Kaye, Olivia Stiehl, Peter J Foster, Michael J Shelley, Daniel J Needleman, and Sebastian Fürthauer. Measuring and modeling polymer concentration profiles near spindle boundaries argues that spindle microtubules regulate their own nucleation. *New Journal of Physics*, 20(5):055012, 2018.
- [51] Franziska Decker, David Oriola, Benjamin Dalton, and Jan Brugués. Autocatalytic microtubule nucleation determines the size and mass of xenopus laevis egg extract spindles. *Elife*, 7:e31149, 2018.
- [52] Akanksha Thawani, Rachel S Kadzik, and Sabine Petry. Xmap215 is a microtubule nucleation factor that functions synergistically with the γ -tubulin ring complex. *Nature cell biology*, 20(5):575–585, 2018.
- [53] Akanksha Thawani, Howard A Stone, Joshua W Shaevitz, and Sabine Petry. Spatiotemporal organization of branched microtubule networks. *Elife*, 8:e43890, 2019.
- [54] Stefanie Redemann, Sebastian Fürthauer, Michael Shelley, and Thomas Müller-Reichert. Current approaches for the analysis of spindle organization. *Current opinion in structural biology*, 2019.
- [55] Stefanie Redemann, Ina Lantzsch, Norbert Lindow, Steffen Prohaska, Martin Srayko, and Thomas Müller-Reichert. A switch in microtubule orientation during *c. elegans* meiosis. *Current Biology*, 28(18):2991–2997, 2018.
- [56] Ina Lantzsch, Che-Hang Yu, Hossein Yazdhkasti, Norbert Lindow, Erik Szentgyoergyi, Steffen Prohaska, Martin Srayko, Sebastian Fuerthauer, and Stefanie Redemann. Microtubule re-organization during female meiosis in *c. elegans*. *BioRxiv*, 2020.
- [57] Nenad Pavin, Liedewij Laan, Rui Ma, Marileen Dogterom, and Frank Jülicher. Positioning of microtubule organizing centers by cortical pushing and pulling forces. *New Journal of Physics*, 14(10):105025, 2012.
- [58] Ehsan Nazockdast, Abtin Rahimian, Daniel Needleman, and Michael Shelley. Cytoplasmic flows as signatures for the mechanics of mitotic positioning. *Molecular biology of the cell*, 28(23):3261–3270, 2017.
- [59] Reza Farhadifar, Che-Hang Yu, Gunar Fabig, Hai-Yin Wu, David B Stein, Matthew Rockman, Thomas Müller-Reichert, Michael J Shelley, and Daniel J Needleman. Stoichiometric interactions explain spindle dynamics and scaling across 100

- million years of nematode evolution. *Elife*, 9:e55877, 2020.
- [60] Taylor Sulerud, Abdullah Bashar Sami, Guihe Li, April Kloxin, John Oakey, and Jesse Gatlin. Microtubule-dependent pushing forces contribute to long-distance aster movement and centration in *xenopus laevis* egg extracts. *Molecular Biology of the Cell*, 31(25):2791–2802, 2020.
- [61] Johnathan L Meaders and David R Burgess. Microtubule-based mechanisms of pronuclear positioning. *Cells*, 9(2):505, 2020.
- [62] Jing Xie and Nicolas Minc. Cytoskeleton force exertion in bulk cytoplasm. *Frontiers in cell and developmental biology*, 8:69, 2020.
- [63] James F Pelletier, Christine M Field, Sebastian Fürthauer, Matthew Sonnett, and Timothy J Mitchison. Co-movement of astral microtubules, organelles and f-actin by dynein and actomyosin forces in frog egg cytoplasm. *Elife*, 9:e60047, 2020.
- [64] Tim Sanchez, Daniel TN Chen, Stephen J DeCamp, Michael Heymann, and Zvonimir Dogic. Spontaneous motion in hierarchically assembled active matter. *Nature*, 491(7424):431–434, 2012.
- [65] F. Keber, E. Loiseau, T. Sanchez, S. DeCamp, L. Giomi, M. Bowick, M. Marchetti, Z. Dogic, and A. Bausch. Topology and dynamics of active nematic vesicles. *Science*, 345:1135–1139, 2014.
- [66] Achini Opathalage, Michael M Norton, Michael PN Juniper, Blake Langeslay, S Ali Aghvami, Seth Fraden, and Zvonimir Dogic. Self-organized dynamics and the transition to turbulence of confined active nematics. *Proceedings of the National Academy of Sciences*, 116(11):4788–4797, 2019.
- [67] Pooja Chandrakar, Minu Varghese, S Ali Aghvami, Aparna Baskaran, Zvonimir Dogic, and Guillaume Duclos. Confinement controls the bend instability of three-dimensional active liquid crystals. *Physical Review Letters*, 125(25):257801, 2020.
- [68] Simon Čopar, Jure Aplinc, Žiga Kos, Slobodan Žumer, and Miha Ravnik. Topology of three-dimensional active nematic turbulence confined to droplets. *Physical Review X*, 9(3):031051, 2019.
- [69] Guillaume Duclos, Raymond Adkins, Debarghya Banerjee, Matthew SE Peterson, Minu Varghese, Itamar Kolvin, Arvind Baskaran, Robert A Pelcovits, Thomas R Powers, Aparna Baskaran, et al. Topological structure and dynamics of three-dimensional active nematics. *Science*, 367(6482):1120–1124, 2020.
- [70] Shiladitya Banerjee, Margaret L Gardel, and Ulrich S Schwarz. The actin cytoskeleton as an active adaptive material. 2020.
- [71] Peter J Foster, Sebastian Fürthauer, Michael J Shelley, and Daniel J Needleman. Active contraction of microtubule networks. *eLife*, page e10837, 2015.
- [72] Peter J Foster, Wen Yan, Sebastian Fürthauer, Michael J Shelley, and Daniel J Needleman. Connecting macroscopic dynamics with microscopic properties in active microtubule network contraction. *New Journal of Physics*, 19(12):125011, 2017.
- [73] Daniel Needleman and Zvonimir Dogic. Active matter at the interface between materials science and cell biology. *Nature Reviews Materials*, 2(9):1–14, 2017.
- [74] Paul M Chaikin and Tom C Lubensky. Principles of condensed matter physics, 2000.
- [75] Karsten Kruse, Alexander Zumdieck, and Frank Jülicher. Continuum theory of contractile fibres. *EPL (Europhysics Letters)*, 64(5):716, 2003.
- [76] Tanniemola B Liverpool and M Cristina Marchetti. Rheology of active filament solutions. *Physical review letters*, 97(26):268101, 2006.
- [77] Julio M Belmonte, Maria Leptin, and François Nédélec. A theory that predicts behaviors of disordered cytoskeletal networks. *Molecular Systems Biology*, 13(9):941, 2017.
- [78] David Saintillan and Michael J Shelley. Instabilities and pattern formation in active particle suspensions: kinetic theory and continuum simulations. *Physical Review Letters*, 100(17):178103, 2008.
- [79] David Saintillan and Michael J Shelley. Instabilities, pattern formation, and mixing in active suspensions. *Physics of Fluids*, 20(12):123304, 2008.
- [80] Ganesh Subramanian and Donald L Koch. Critical bacterial concentration for the onset of collective swimming. *Journal of Fluid Mechanics*, 632:359, 2009.
- [81] Aparna Baskaran and M Cristina Marchetti. Statistical mechanics and hydrodynamics of bacterial suspensions. *Proceedings of the National Academy of Sciences*, 106(37):15567–15572, 2009.
- [82] G. Batchelor. Slender-body theory for particles of arbitrary cross-section in stokes flow. *J. Fluid Mech.*, 44:419–440, 1970.
- [83] R Aditi Simha and Sriram Ramaswamy. Hydrodynamic fluctuations and instabilities in ordered suspensions of self-propelled particles. *Physical review letters*, 89(5):058101, 2002.
- [84] Barath Ezhilan, Michael J Shelley, and David Saintillan. Instabilities and nonlinear dynamics of concentrated active suspensions. *Physics of Fluids*, 25(7):070607, 2013.
- [85] C. Hohenegger and M. Shelley. Stability of active suspensions. *Phys. Rev. E*, 81:046311, 2010.
- [86] D. Saintillan and M. Shelley. Active suspensions and their nonlinear models. *C. R. Phys.*, 14:497–517, 2013.
- [87] T. Gao, R. Blackwell, M. Glaser, M. Betterton, and M. Shelley. Multiscale modeling and simulation of microtubule/motor protein assemblies. *Phys. Rev. E*, 92:062709, 2015.
- [88] Joseph B Keller and Sol I Rubinow. Slender-body theory for slow viscous flow. *Journal of Fluid Mechanics*, 75(4):705–714, 1976.
- [89] Robert Blackwell, Oliver Sweezy-Schindler, Christopher Baldwin, Loren E Hough, Matthew A Glaser, and MD Betterton. Microscopic origins of anisotropic active stress in motor-driven nematic liquid crystals. *Soft Matter*, 12(10):2676–2687, 2016.
- [90] Tanniemola B Liverpool and M Cristina Marchetti. Hydrodynamics and rheology of active polar filaments. In *Cell motility*, pages 177–206. Springer, 2008.

- [91] G. Yang, L. Cameron, P. Maddox, E. Salmon, and G. Danuser. Regional variation of microtubule flux reveals microtubule organization in the metaphase meiotic spindle. *J. Cell Bio.*, 182:631–639, 2008.
- [92] Hajer Ennomani, Gaëlle Letort, Christophe Guérin, Jean-Louis Martiel, Wenxiang Cao, François Nédélec, M Enrique, Manuel Théry, and Laurent Blanchoin. Architecture and connectivity govern actin network contractility. *Current Biology*, 26(5):616–626, 2016.